IEEE Access
Multidisciplinary | Rapid Review | Open Access Journal

Received 15 October 2022, accepted 29 November 2022, date of publication 9 December 2022, date of current version 22 December 2022.

Digital Object Identifier 10.1109/ACCESS.2022.3228043

RESEARCH ARTICLE

Utilizing Non-Orthogonal Polarization With Polarization Reuse Technique for 4 × 4 MIMO Capacity Enhancement

LAXMIKANT MINZ[1], YE-EUN CHI[1], KYUNGHOON KWON[2], MIN-SEON YUN[2], YOUNG-CHAN MOON[2], DUK-YONG KIM[2], AND SEONG-OOK PARK[1], (Senior Member, IEEE)

[1]Microwave and Antenna Laboratory, Department of Electrical Engineering, KAIST, Daejeon 34141, South Korea
[2]KMW Inc., Hwaseong 18462, South Korea

Corresponding author: Laxmikant Minz (lkminz@kaist.ac.kr)

This research was supported by BK21 FOUR and the KMW Inc.(Project No. G01200424, Channel capacity increase technique and channel model analysis of OPRA technology).

ABSTRACT 5G communication promises fast and large data stream which requires higher capacity of a cellular wireless network. A higher capacity could be achieved with wider bandwidth and network densification, but they are expensive approaches. Instead, upgrading the wireless network with higher-order Multiple Input Multiple Output (MIMO) antenna system with polarization diversity can inexpensively escalate the peak data rate for higher capacity. We present a 4 × 4 MIMO cellular network scheme utilizing polarization reuse and using 4 polarization to reform the cellular network from current state of the art of dual polarization 4 × 4 MIMO scheme. 4 Polarization (vertical, Horizontal, ±45° slant) is used in 2 orthogonal polarization pair form, with a beam-separation among pair, to intensify polarization diversity and maximize the MIMO network channel capacity. This beam-separated polarization reuse technique minimizes the channel correlation which maximizes the probability of four independent data streams (rank 4). The simulated result of the channel capacity with the proposed scheme achieves a 30% higher capacity compared to the baseline configuration of 3-sector 4 × 4 MIMO. The field trial of the presented network indicates a higher portion of rank 4, supporting four independent data streams in the rich scattering environment of a cellular network.

INDEX TERMS 4 × 4 MIMO, 5G, 4T4R, channel capacity, dual beam, multiple polarization, polarization diversity, polarization reuse, rank index.

I. INTRODUCTION

The wireless communication network is evolving and currently 5G networks are being deployed with higher data rates (expected speed of 100 Gb/s) with better quality wireless signals. There are three basic techniques to achieve high data rate in a cellular network - by utilizing wider bandwidth [1], [2], by having more cells (or sites) on an existing network [3], [4], or by improving spectrum efficiency [5], [6], [7]. Increasing the channel bandwidth is an effective and direct approach to increase network capacity, however, the spectrum is very limited, so it is not convenient to use wider bandwidth. The other method of adding more sites is both difficult and an expensive approach, especially in urban areas. Nonetheless, improving spectrum efficiency is a cost-effective technique to increase the network capacity. A promising way of achieving a high data rate is to use multiple antennas at both the transmitter and the receiver side in a wireless communications network, forming a multiple-input multiple-output (MIMO) system.

MIMO system offers spatial diversity and spatial multiplexing which substantially improves network capacity and spectral efficiency without utilizing more bandwidth and more total system power [8], [9], [10]. In addition to

The associate editor coordinating the review of this manuscript and approving it for publication was Emrecan Demirors.

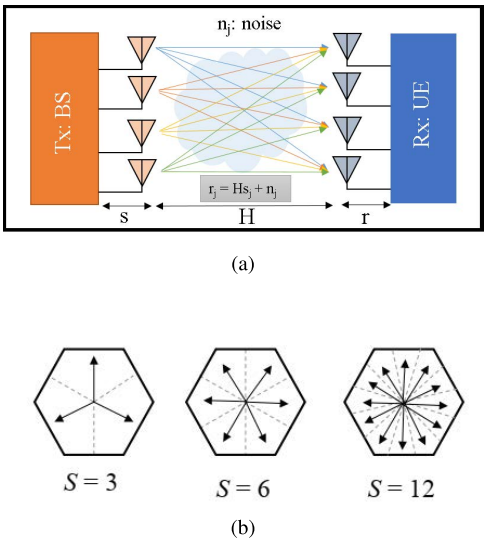

FIGURE 1. Spectral efficiency enhancement using (a) MIMO technique, (b) site sectorization technique.

MIMO system, another cost-effective and practical means of improving spectral efficiency, and consequently enhancing network capacity, is the sectorization of the site, where each site is partitioned into multiple sectors and spectral resources are reused in each sector [11], [12], [13], [14]. A view of MIMO technique and site sectorization technique is shown in Fig. 1.

In MIMO system, multiple parallel sub-channels can be established between the transmitter and the receiver antennas which leads to spectral efficiency if the fading of the transmitter-receiver pairs is uncorrelated. There is a linear increase in capacity with the increase in number of antennas in MIMO system. Therefore, massive MIMO is being considered for 5G communication to increase network capacity, improve coverage, and provide better user experience of fast and large data streams [15], [16], [17]. Massive MIMO is the extension of MIMO using 100s of antenna elements with all the advantages of conventional MIMO on a greater scale. However, the complexity of implementing MIMO operation and antenna panel on Base Station (BS) or User Equipment (UE), as well as the cost, scaled up with massive MIMO. Alternatively, without increasing the transceiver array's space, the number of communication channels can be increased by utilizing multiple polarization antennas. Exploitation of polarization diversity in MIMO has been utilized to reduce correlation and maximize channel capacity with more antennas in a compact space [18], [19], [20]. A Cross-polarized systems are able to double the antenna numbers, hence the channel capacity, for half the space needed for co-polarized antennas. A cross-polarized MIMO system is limited to 2 polarization, orthogonal to each other. A further increase in the MIMO capacity could be expected with greater number of polarization signal (more than two polarization). Such schemes were proposed and tested in [21] and [22], however, multiple polarization channel could not be orthogonal to each other and therefore could have high correlation, which will severely degrade the channel capacity. A signal separation algorithm using priory signal information is suggested in [21] to use multiple polarization communication. In the literature, there are very few studies on the use of more than 2 polarization in MIMO system.

Here in this paper, polarization reuse scheme is introduced to use more than two polarization with low correlation and enhance the overall network capacity. This novel polarization reuse approach is motivated from the principle of frequency reuse scheme. In frequency reuse, the sectors that use the same set of frequencies are separated from one another by a large distance to avoid co-channel interference. Similarly, optimally beam-separated antenna power pattern scheme of non-orthogonal polarization covering a base station (BS) sector can be used to reduce spatial correlation between non-orthogonal polarization channel and make it practically feasible to use multiple polarization in MIMO cellular communication. This beam-separated scheme of multiple polarization over a sector if applied to entire BS cell can be recognized as polarization reuse scheme.

In this paper, a new 3-sector 4T4R (4 transmitters and 4 receivers antenna, 4 × 4 MIMO) base station cell configuration is proposed and designed for 5G cellular network with polarization reuse scheme. A 3-sector 4T4R configuration consist of 2 orthogonal polarization antenna array, is a widely deployed configuration in present cellular network, considered henceforth as baseline antenna configuration. We examine 4 polarization (vertical, horizontal, +45°/−45° slant polarization) usages for 4 transmitter of 4T4R MIMO system for higher capacity over the sector in a cellular network. In our proposed scheme, each sector of a 3-sector site is covered using 2 distinct cross-polarization pair (V/H and +45° /−45°) with optimized beam separation among distinct cross-polarization pair radiation pattern. The beam-separated cross-polarized dual beam scheme virtually convert the 3-sector site into 6-sector site without the high-order sectorization disadvantages and aid in improving spectral efficiency. We employed 2 distinct cross-polarization with beam separate which results in higher capacity with frequency coverage equivalent to baseline configuration and with same number of the antennas as in baseline configuration. This technique is categorized as orthogonal polarization reuse (OPR) and the antenna system employed for this technique can be called orthogonal polarization reuse antennas (OPRA). The channel simulation with the proposed OPRA configuration shows a 30% increase in peak and average capacity compared to baseline configuration. We also performed the field trial test of the proposed scheme of multiple orthogonal polarization reuse and the measured result shows a higher proportion of rank 4 (4 independent data stream) in a sector compared to baseline scheme. The proposed system also provides a higher capacity of 4 × 4 MIMO compared to the baseline system.

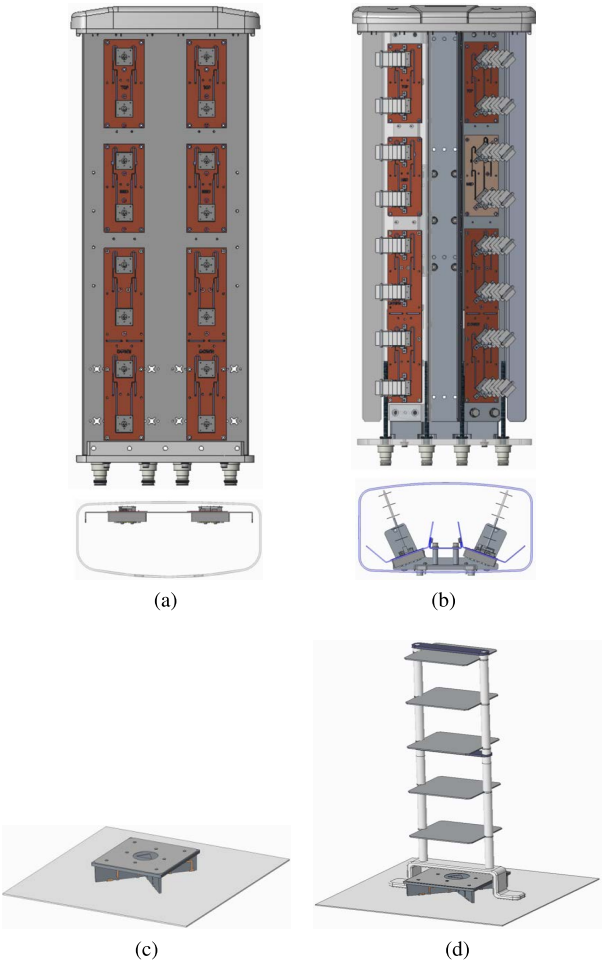

FIGURE 2. Front and top view of BS MIMO antenna panel (a) Baseline configuration. (b) Proposed dual beam configuration with orthogonal polarization reuse. (c) Baseline antenna element closeup (d) OPRA element closeup.

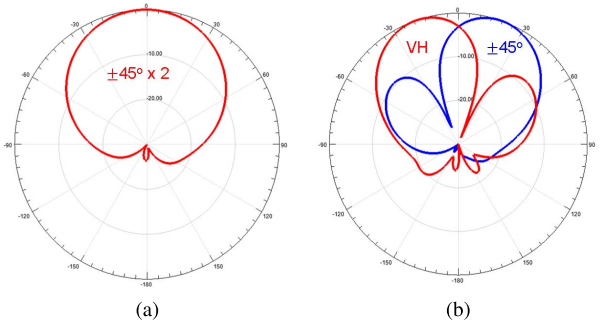

FIGURE 3. Radiation pattern of (a) Baseline antenna configuration (b) Proposed twin beam pattern with orthogonal polarization reuse.

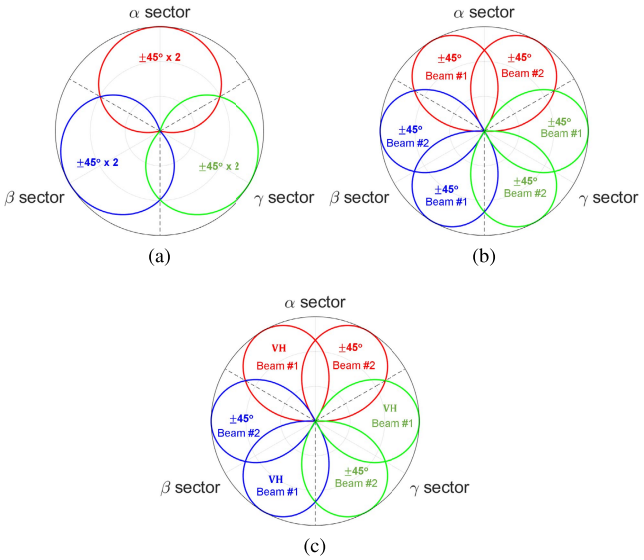

FIGURE 4. Cell sectorization and coverage in (a) Baseline configuration (b) Twin beam same polarization (c) Proposed dual beam with OPRA.

The paper is arranged as follows. The details of the antenna unit and OPRA antenna configuration with dual beam for a sector is presented in section II. 3D polarized channel modelling details are given in section III. OPRA configuration analysis is presented in section IV and section V shows the simulation performance of the proposed model. Section VI presents the field trial test of the proposed 4T4R multiple orthogonal polarization reuse cellular network scheme. Finally, conclusions are drawn in section VII.

II. ORTHOGONAL POLARIZATION REUSE ANTENNA SYSTEM

We developed same size polarized antenna BS panels with a single beam and dual beam radiation pattern for 4T4R 3-sector site (120° each). The model of baseline antenna panel and OPRA panel consist of cross-polarized L probe fed patch antenna, shown in Fig. 2 and the respective normalized radiation patterns of panels are shown in Fig. 3. The L probe fed patch is used to have wider bandwidth antenna for 5G network. The baseline and proposed BS antenna panel, both consists of an array of 2 cross-polarized patch antennas for 4 × 4 MIMO cellular network. In the proposed BS panel 2 cross-polarized arrays are rotated symmetrically away from panel's broadside direction to form beam-separated dual beam, Fig. 2(b). Moreover, for the polarization reuse, the dual beam are formed from different set of cross-polarization, vertical/horizontal (V/H) and +45°/−45° polarization, by changing the orientation of antenna element. The dual beams can also be formed using same cross-polarization without change in antenna element orientation (called as twin beam scheme henceforth), which is considered in our study for comparison with proposed BS panel. In twin Beam scheme, site sectorization is similar to the proposed orthogonal polarization reuse BS, but the dual beam is formed using the same cross-polarization, +45°/−45° polarization, and therefore polarization reuse is not supported by it. A cellular network site coverage with baseline configuration, Twin Beam, and the proposed OPRA system is shown in Fig. 4. The 3-sector are named α, β, γ in Fig. 4. These 3 configurations are used for our experiment, analysis, and comparison.

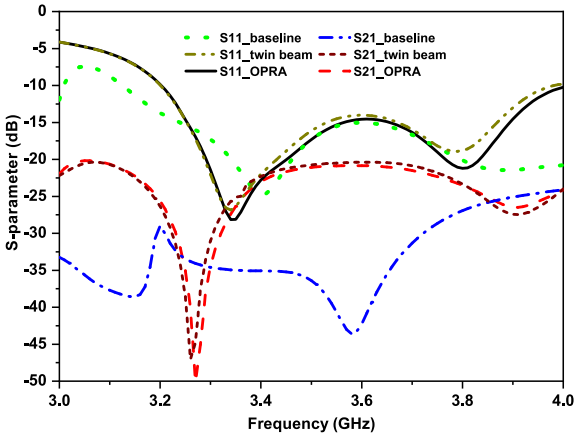

FIGURE 5. S-parameter of baseline antenna, Twin beam same polarization antenna, and OPRA.

The dual beam pattern of OPRA with different pair of orthogonal polarization appears to virtually double the number of the sector of a site without the associated drawback of higher sectorization. In the multiple orthogonal polarization reuse, the system uses same frequency channel over 120° sector (same as baseline antenna configuration, $\alpha/\beta/\gamma$). Therefore, truncation efficiency over 120° sector, which depends on available frequency channels and decreases with higher sectorization, would not decrease with the proposed OPRA system compared to the baseline configuration. As the frequency coverage over a site does not decrease with multiple orthogonal polarization reuse, the number of handoffs in the cellular network will also not increase compared to the baseline configuration. The sectorization drawbacks exist with the Twin beam same polarization BS system (Fig.4(b)), where each beam has the same cross-polarization field. Further, there will be high channel correlation over the overlapping field zone between two beams in Twin beam BS system. The higher correlation reduces the capacity of the network for Twin beam BS system. The proposed OPRA system has a minimum correlation among the dual beams due to different orthogonal cross-polarization. A detail analysis of the Twin beam and proposed OPRA system is presented in the following section.

In the baseline BS antenna panel, dual-polarized antennas have radiation pattern of beamwidth 65° in broadside direction, Fig. 3(a). The OPRA system has a dual beam, each of 40° beamwidth, Fig. 3(b). The cross-polarized antenna in the proposed OPRA system is loaded with directors, Fig. 2(d), which provides high gain, suitable beamwidth, and lower sidelobe level to the OPRA system radiation pattern. The designed antenna systems are an array of 8 elements and the gain of the baseline and proposed system is 17.5 dBi and 19.5 dBi, respectively. The reflection coefficient of the designed baseline antenna array, conventional twin beam same polarization array and, proposed OPRA antenna array is shown Fig. 5. All designed antenna configurations have -10 dB reflection coefficient from 3.2 GHz to 4 GHz. They are designed to perform the field test measurement at 3.5 GHz with 100 MHz bandwidth for our study. The isolation between the two cross-polarization antenna port, shown as S21 in Fig. 5, is well below -20 dB for baseline, Twin beam as well as OPRA array configuration. The S-parameter characteristics of Twin beam same polarization array is similar to OPRA system. All three BS panels are designed and fabricated for the field test measurement and comparison of capacity over the sector $\alpha/\beta/\gamma$. The Proposed BS antenna panel is of the same size as the baseline antenna panel, therefore the BS pole, frame, and system arrangement need not be changed, incurring no additional installation or setup cost.

III. POLARIZED 3D MIMO CHANNEL MODELLING & FORMULATION

The spatial channel models (SCM) are mathematically simple model among several channel models. Therefore, it is easy to develop and implement SCM but at the same time often realistic behaviour of the propagation channel is compromised. In contrary, a geometry based stochastic channel model, where channel properties are described by statistical distribution, usually provide real environment channel by a sum of multipath components [23]. In this paper, in order to verify the working of proposed 4 polarization MIMO system, we analyse 4 polarization MIMO system using SCM due to its mathematical simplicity. The equations and details of the 3D SCM, a modified model from previous work [24], is presented in this section. However, we used COST 259 channel model (geometry based stochastic channel model) in section V for simulation and evaluation of proposed OPRA system with the real environment (urban) channel characteristics for comparison with field trial test results.

Spatial channel models (SCM) are developed to represent MIMO links by considering antenna array geometries and antenna array responses. Earlier SCMs (2D models) are simplified by considering that propagating wave arrives only from azimuth plane [25], [26], [27], however, it has been found that arrival/departure of wireless signal in both azimuth and elevation plane is significant for cross correlation analysis between polarized antennas in MIMO system [28], [29], [30], therefore, a 3D SCM considering wave propagation both in azimuth and elevation plane is essential for accurate analysis of multi-polarized MIMO system. Accordingly, a two sphere 3D geometrical SCM [24] is considered in this paper with antenna polarization and channel depolarization for the 4 polarization OPRA configuration analysis. In this spherical model a 3D Von Mises Fisher (VMF) directional distribution of scatterers are considered over the sphere to closely emulate the real environment scatterer measurement data to fully create a 3D channel model. This 3D VMF distributions are flexible and also allow modelling dependence between AoAs and AoDs [31]. An important update in the considered channel model is to also consider full 3D antenna responses to completely suit

the multi-polarization MIMO analysis. This can be achieved by describing the antenna response vector in it's θ and ϕ components. The channel transfer function of a polarized MIMO system, described in 3GPP standards [32], with 3D antenna response, 3D VMF scatterer distribution, and infinite number of scatterer K and L at Tx and Rx, respectively, in the context of considered 3D geometric model can be formulated in integral form as:

$$\begin{aligned} h_{u,s}(t) = \sqrt{P_{us}} \iint_{\Omega^{\mathrm{Tx}}} \iint_{\Omega^{\mathrm{Rx}}} exp(-jk_0(D_{su}))t \\ \times \left[F_s^{Tx}(\Omega^{Tx})\right]^T \times \left[\overline{A}\right] \times \left[F_u^{Rx}(\Omega^{Rx})\right] \\ \times p^{\mathrm{Tx}}(\Omega^{\mathrm{Tx}}) p^{\mathrm{Rx}}(\Omega^{\mathrm{Rx}}) exp(j\mathbf{k_1}\mathbf{v}t) d\Omega^{\mathrm{Tx}} d\Omega^{\mathrm{Rx}} \end{aligned} \quad (1)$$

where P_{us} is the power transferred through the $\mathrm{Tx}_s - \mathrm{Rx}_u$ sub-channel, D_{su} is overall distance between $\mathrm{Tx}_s - \mathrm{Rx}_u$ with unique angle of arrivals (AoA) and angle of departures (AoD) due to scatterer at Tx and Rx, $\mathbf{k_1}$ is the wave vector pointing in the propagation direction from the scatterer. $\mathbf{v}$ is the velocity vector for the moving receiver. $p^{\mathrm{Tx}}(\Omega^{\mathrm{Tx}})$ and $p^{\mathrm{Rx}}(\Omega^{\mathrm{Rx}}$ are the VMF scatterer distributions at the Tx and Rx. $F_s^{Tx}(\Omega_k^{Tx})$ and $F_u^{Rx}(\Omega_k^{Rx})$ are the complex field pattern of sth transmit antenna and uth receive antenna, respectively. For the polarized antenna the field pattern are describe using orthogonal θ and ϕ components

$$F(\Omega) = \begin{bmatrix} F^{(\theta)}(\Omega) \\ F^{(\phi)}(\Omega) \end{bmatrix} \quad (2)$$

$\overline{A}$ is polarization matrix, given as:

$$\overline{A} = \begin{bmatrix} exp(j\Phi_{l,k}^{(\theta\theta)}) & \sqrt{\kappa}\sqrt{\chi}exp(j\Phi_{l,k}^{(\theta\phi)}) \\ \sqrt{\kappa}exp(j\Phi_{l,k}^{(\phi\theta)}) & \sqrt{\chi}exp(j\Phi_{l,k}^{(\phi\phi)}) \end{bmatrix} \quad (3)$$

where $\Phi_{l,k}^{x,y}$ is phase shift between x polarized transmit antenna and y polarized receive antenna due to the interaction of the local scatterers k and l. They are assumed independent and identically distributed (i.i.d.) random variables following the uniform distribution over $[0, 2\pi]$. The 2×2 matrix, $\overline{A}$, represents the scattering phases and amplitudes of a plane wave leaving the $\mathrm{Tx_s}$ with a given angle and polarization and arriving $\mathrm{Rx_u}$ with another direction and polarization. κ is the average power ratio of waves leaving the $\mathrm{Tx_s}$ in the spherical basis vector $\hat{\theta}$ direction and arriving at $\mathrm{Rx_u}$ in the spherical basis vector $\hat{\phi}$ direction to those arriving at Rx_u in the spherical basis vector $\hat{\theta}$ direction. By symmetry the power ratio of the opposite process ($\hat{\phi}$-$\hat{\theta}$ over $\hat{\phi}$-$\hat{\phi}$) is chosen to be the same. k is the inverse cross-polar discrimination (XPD). χ is the inverse of the co-polar ratio (CPR).

Based on (1)-(3) any channel response between Tx and Rx antenna of any polarizations (same, orthogonal, or random) can be evaluated, which is used to measure MIMO system characteristics such as correlation and capacity. The spatial correlation between two channel, say $h_{u,s}$ (between $\mathrm{Tx_s} - \mathrm{Rx_u}$) and $h_{p,q}$ (between $\mathrm{Tx_q} - \mathrm{Rx_p}$) denoted as $r_{pq,us}(t)$ such as [33]

$$\begin{aligned} r_{pq,us}(t) &= E[h_{p,q}^{norm}(t)h_{u,s}^{norm*}(t)] \\ &= \frac{E[h_{p,q}(t)h_{u,s}^{*}(t)]}{\sqrt{E\left|h_{p,q}(t)\right|^2}\sqrt{E\left|h_{u,s}(t)\right|^2}} \end{aligned} \quad (4)$$

where $E[h_{p,q}^{norm}(t)h_{u,s}^{norm*}(t)]$ can be derived from (1) in integral form as:

$$\begin{aligned} E[h_{p,q}^{norm}(t)h_{u,s}^{norm*}(t)] \\ = \sqrt{P_{us}P_{pq}} \iint_{\Omega^{\mathrm{Tx}}} \iint_{\Omega^{\mathrm{Rx}}} exp(-jk_0(D_{su} - D_{qp}))t \\ \times \left[F_s^{Tx}(\Omega^{Tx})\right]^T \times \left[\overline{A}\right] \times \left[F_u^{Rx}(\Omega^{Rx})\right] \\ \times \left[F_q^{Tx}(\Omega^{Tx})\right]^T \times \left[\overline{-A}\right] \times \left[F_p^{Rx}(\Omega^{Rx})\right] \\ \times p^{\mathrm{Tx}}(\Omega^{\mathrm{Tx}}) p^{\mathrm{Rx}}(\Omega^{\mathrm{Rx}}) exp(j\mathbf{k_1}\mathbf{v}t) d\Omega^{\mathrm{Tx}} d\Omega^{\mathrm{Rx}} \end{aligned} \quad (5)$$

$r_{pq,us}(t)$ is one of the element of MIMO correlation matrix, $\mathbf{R}$. It is found that the spatial correlation matrix coefficient $r_{i,j}$ is equal to its conjugate, $r_{j,i}$, where $i \neq j$ and that $r_{i,i}$ is unity. Therefore, the spatial correlation of the MIMO system can be evaluated by

$$\bar{r} = \frac{\sum_{i<j}\left|r_{i,j}\right|}{US(US-1)/2} \quad (6)$$

where U is the number of antenna at Tx side and S is the number of antenna at Rx side. From correlation matrix, we can generate channel impulse response matrix as

$$\mathbf{H} = unvec(\mathbf{R}^{1/2}vec(\mathbf{H_w})) \quad (7)$$

where $\mathbf{H_w}$ is matrix with complex Gaussian elements. The channel matrix $\mathbf{H}$ incorporate spatial correlation characteristics. It is assumed that the transmitter has no channel state information and only the receiver knows channel realization. This implies that the signals are independent and the power is equally divided among the transmit antennas. For this condition, the capacity of MIMO channel is given by:

$$C = log_2\left[det\left(\mathbf{I} + \frac{\rho}{S}\mathbf{H}\mathbf{H}^T\right)\right] \quad (8)$$

where $\mathbf{I}$ is UxU identity matrix and $\mathbf{H}$ is the normalized channel matrix (computed by (7)), ρ is the average signal-to-noise ratio (SNR). SNR can be calculated based on Radio Unit (RU) transmit power, system noise figure, and pathloss as:

$$SNR(dB) = P_{tx} + G_{tx} - PL + G_{UE} - N_{tn} - L_n \quad (9)$$

where P_{tx} is BS output power (52 dBm), G_{tx} is Tx gain, G_{UE} is UE antenna gain, PL is path loss, N_{tn} is thermal noise (-174 dBm/Hz), L_n is noise figure (7 dB). The path loss for NLOS (Non-Line Of Sight) according to 3GPP TR38.901 UMa formulated as [34]:

$$\begin{aligned} PL'_{UMa-NLOS} = 13.54 + 39.08log_{10}(d_{3D}) \\ + 20log_{10}(f_c) - 0.6(h_{UE} - 1.5) \end{aligned} \quad (10)$$

where d_{3D} is the 3D distance between the BS and UE.

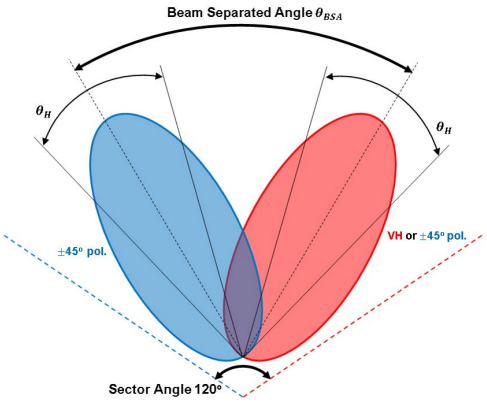

FIGURE 6. Beam separated angle view.

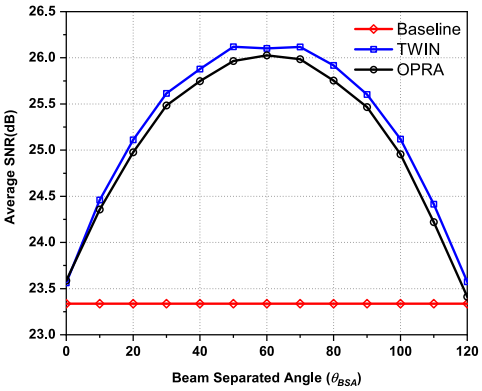

FIGURE 7. Avg. SNR plot over a sector with respect to θ_{BSA}.

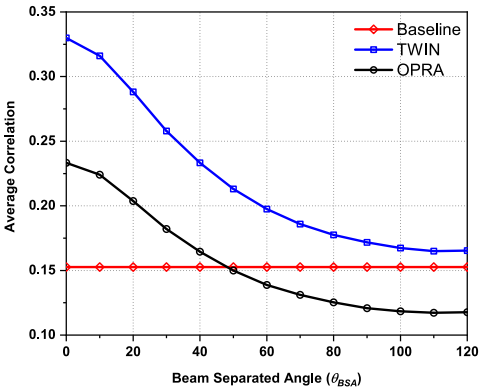

FIGURE 8. Avg. correlation plot over a sector with respect to θ_{BSA}.

IV. OPRA CONFIGURATION ANALYSIS

In the OPRA scheme, there are two beams of 2 different orthogonal polarization pair (V/H and +45°/−45°), separated at an angle for maximum capacity. In this section, the OPRA's dual beam separation analysis in comparison to Twin beam same polarization scheme and baseline scheme is presented. For the simulation and comparison, normalized field pattern of the different schemes (Fig. 3) is considered as Tx antenna pattern. Whereas a simple cross-polarized (V/H) omnidirectional dipole antenna as in [24] is considered for

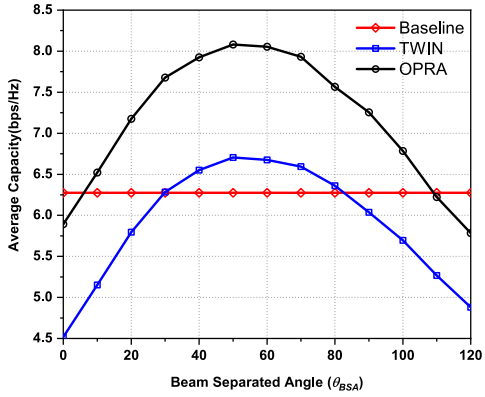

FIGURE 9. Avg. capacity plot over a sector with respect to θ_{BSA}.

the Rx antenna unit. Also we set $d_T = 0.5\lambda$, $d_R = 0.5\lambda$, $\phi_{Rx} = 0°, \theta_{Rx} = 90°$, the mean $XPD = 9$ dB, and mean $CPR = 5$ dB.

For analysis, the dual beams of OPRA and of Twin beam same polarization configuration are separated in angle, θ_{BSA}, from 0° (completely overlapping) to 120° (extent of a sector) angles and compared in terms of average SNR, capacity, and correlation. The beam separation view of the dual beam for OPRA and Twin beam with same polarization is shown in Fig. 6. The left and right beams are of different orthogonal polarization set in case of OPRA and of same orthogonal polarization set (+45°/−45°) for Twin beam same polarization case. The analysis is made by uniformly distributed 500,000 random samples within a sector (−60° to 60° and 0 to 500 m) at different θ_{BSA}.

The simulated average SNR, average correlation, and average capcity vs θ_{BSA} is shown in Fig. 7, Fig. 8, and Fig. 9, respectively. Baseline configuration data is added in the plot for comparison and it remain identical as it is a single beam-direction scheme, not affected with beam separation (θ_{BSA}). SNR at different Rx position is obtained through (9). The average SNR over a sector tends to increase with multiple main beam pointing at differnet directions due to spatial diversity, Fig. 7. However, the SNR gain decline with higher angular beam separation as separate beams became independent with less overlapping, reducing the average received power levels over the sector. The avg. SNR vs θ_{BSA} trend is similar for Twin beam and OPRA configuration. On the contrary, correlation relation with the θ_{BSA}, Fig. 8, is highest for completely overlapped beams and reduces as the θ_{BSA} increases. The spatial correlation among 4 channels between 4Tx and 4Rx, calculated as per (6), became more independent as the beam spearation increases, therefore the correlation became smaller with more beam separation. The phenomenon is very similar to decrease of correlation with more separation between the Tx antennas [24]. Moreover, from the simulation result, the channel correlation for the proposed OPRA configuration is found to be smaller compared to the Twin beam configuration. The reduction in correlation in OPRA is due to usages of 4 different

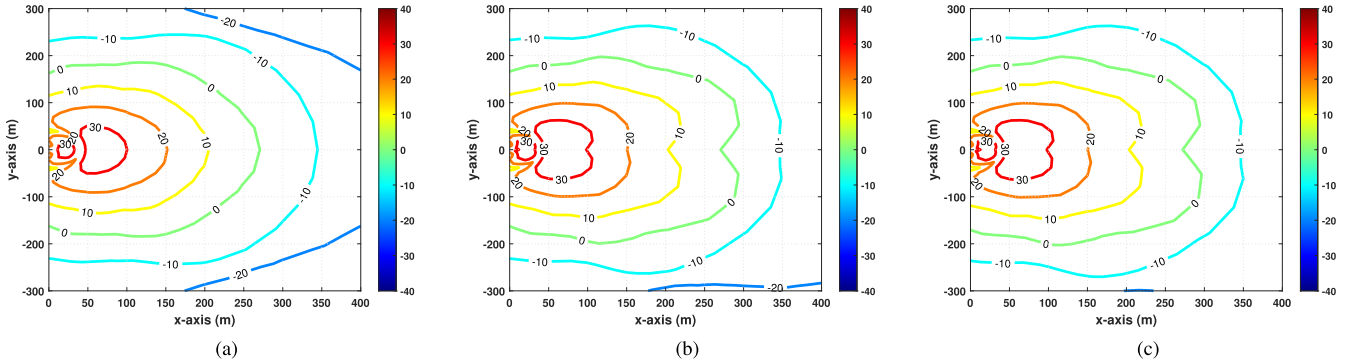

FIGURE 10. SNR distribution of (a) Baseline configuration (b) Twin beam same pol. (c) proposed OPRA system.

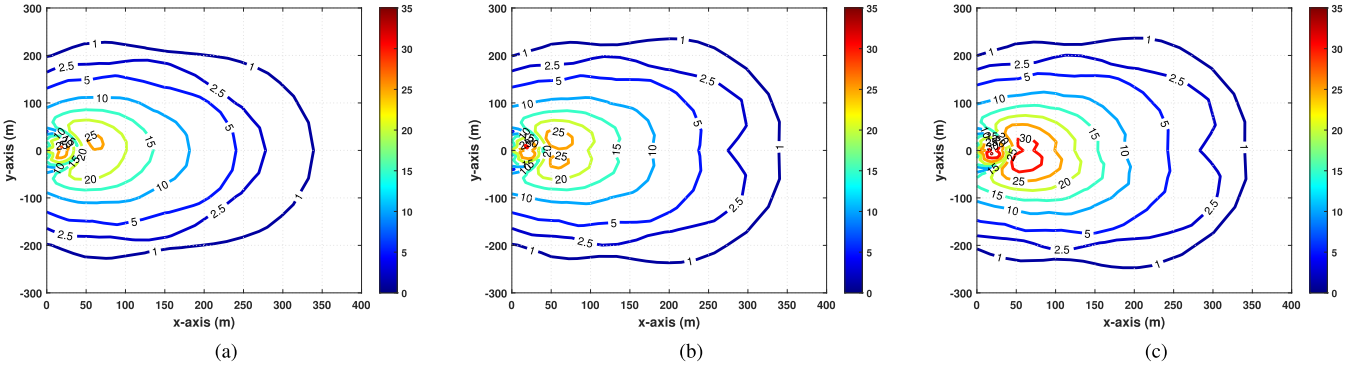

FIGURE 11. Capacity distribution of (a) Baseline configuration (b) Twin beam same pol. (c) proposed OPRA system.

polarization as compared to only two polarization in Twin beam. This is OPRA effect and it shows that channel independence can be guaranteed using different orthogonal polarizations. Nevertheless, the trend of correlation with beam separation for OPRA and Twin beam is same with advantage to OPRA configuration.

SNR and correlation signifcantly affect the capacity of the system. The avg. capacity (bps/Hz) of 4 × 4 MIMO OPRA, Twin beam and baseline configuration with beam separation, calculated from (8), is shown in Fig. 9. The capacity of OPRA and Twin beam, improves with the hihger SNR and smaller correlation. Therefore, despite the similar avg. SNR, the capacity of the OPRA configuration is higher than Twin beam configuration. The OPRA outperform Twin beam by an average of 20%, with maximum difference of 30% at θ_{BSA}=0° and minimum of 18% at θ_{BSA}=120°. The capacity tends to decline with decline in SNR. The analysis with beam separation angle identify the trade-off of correlation and SNR for maximum 4 × 4 MIMO capacity and coverage at $\theta_{BSA} = 40° - 60°$.

In case of a cell composed of three sectors, adjacent sector interference required to be consider, therefore, optimum θ_{BSA} is limited to 40° for the further simulation and field test in subsequent sections. In baseline configuration, there is a single beam covering the sector so its capacity and correlation with beam separation is irrelevant for baseline configuration. For the same Tx and Rx separation and similar other parameters, the baseline average correlation is 0.15 and average capacity is 6.27 bps/Hz over a sector. The above analysis supports the application of polarization reuse for capacity enhancement, also optimum beam separation is analyzed for higher 4 × 4 MIMO capacity performance.

V. SIMULATION RESULT AND DISCUSSION

In the above analysis, we verified the capacity enhancement with proposed OPRA system in comparison to baseline configuration using theoretical 3D Polarized MIMO channel model. In this section simulation with 5G real field scenario is performed. For the simulation, we choose measurement based channel model - COST 259, where angular spread, fading, cluster distribution, cluster size, number of cluster, etc parameters are measured from various measurement campaign in different real environment scenario like urban, semi urban, rural, etc [35]. Some simulation parameters are listed in Table 1.

The simulation and comparison of channel capacity are carried out with 3 types of BS antenna configuration - (1) baseline antenna configuration (4T cross-polarization antenna), (2) 4T Twin beam with same cross-polarization antenna, and (3) the proposed 4T dual beam with different cross-polarized antenna (i.e. OPRA). The second antenna configuration is included to highlight the advantage of

TABLE 1. Simulation parameters.

Items		Value
Carrier Freq. (GHz)		3.5 GHz
Array		8
Scatterer model		COST 259(GTU)
Path loss model		3GPP TR38.901 UMa
# of clusters		6
# of MPCs		20
Tilt angle		10°
# of Tx antenna		4
# of Rx antenna		4
BS antenna spacing	OPRA	λ
	6 sec. same pol. 2 beam	λ
	Baseline antenna	λ
UE antenna spacing		0.5λ (VH&VH, $\oplus\leftrightarrow\oplus$)
# of simulation trials		10000
UE position		-90°∼90°
Distance between BS and UE		0∼500 m
BS antenna height		30 m
Avg building height		15 m
UE height		1.5 m

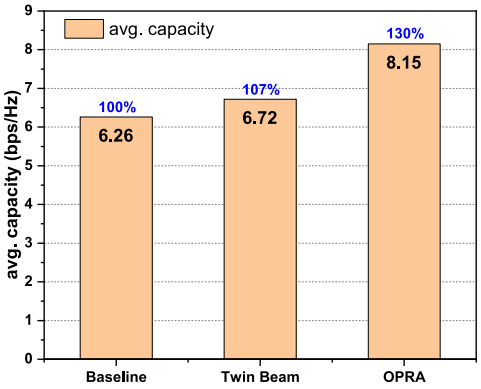

FIGURE 12. Average capacity in a sector (−60°∼60°).

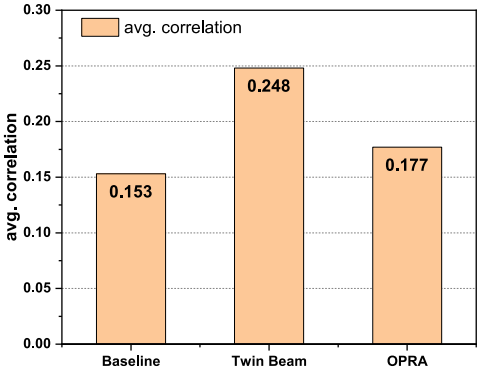

FIGURE 13. Average channel correlation in a sector (−60°∼60°).

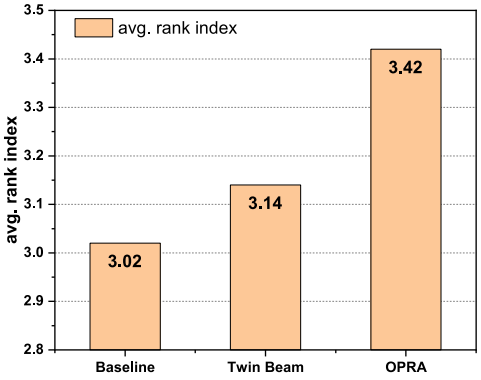

FIGURE 14. Average Rank Index in a sector (−60°∼60°).

OPRA within similar configuration, in addition to baseline configuration. The Tx antennas are 8 element array. In baseline configuration 2 sets of co-located cross-polarized antennas are used for 1 sector and the separation between the 2 sets of antennas used is about λ. The OPRA and twin beam same polarization configuration also uses 2 sets of co-located cross-polarized antenna with separation λ. An angular separation of 40° between the two beams is used as this angle separation was analyzed to provide higher capacity.

In field measurement the UE used was Galaxy Note 10 5G model which support 4 × 4 MIMO 5G NR network. For generalization, 4 omnidirection dipole antennas (same as the Rx antenna in above section analysis) as 2 set of cross-polarization (V/H) is considered in simulation. With 10000 simulation trial, 10000 samples of the channel are generated and MIMO cellular network correlation and capacity is computed as given by (6) and (8).

SNR is an important parameter in (8) which can be calculated for simulation based on 3GPP TR38.901 UMa (Urban Macro) NLOS (Non-Line Of Sight) path loss model formulae (10) using (9). The calculated SNR plot using the path loss, for different antenna configuration is shown in Fig. 10. The SNR is calculated with BS at the center and UE moving away from BS at different angles from −90° to 90° in front covering the sector $\alpha/\beta/\gamma$. The result is then plotted in x-axis and y-axis references by transforming the angular result into 2D plot, shown in Fig 10. The plot shows higher SNR for a short distance and lower SNR for long distance. The SNR is proportional to configuration gain and varies as per the beam pattern of respective configuration.

The channel ergodic capacity of 4 × 4 MIMO for calculated SNR in 2D is shown in Fig. 11. The result is for UE angular position from −90° to 90°. Considering only 1 sector ($\alpha/\beta/\gamma$) of 120° and comparing capacity in −60° to 60° range, OPRA system capacity is observed to be higher than baseline and Twin beam same polarization configuration, especially in the overlapping zone. In the overlapping zone, with the significant SNR, the capacity value for OPRA system is higher for same distance from the BS compared to baseline and Twin beam same polarization system. In that zone, 4 channel with 4 different data streams are maximizing OPRA 4 × 4 MIMO capacity, compared to 4 channels with only 2 polarization in baseline and Twin beam configuration. However, moving away from the overlapping zone towards left or right from BS, the capacity for OPRA, Twin beam, and baseline became similar. There

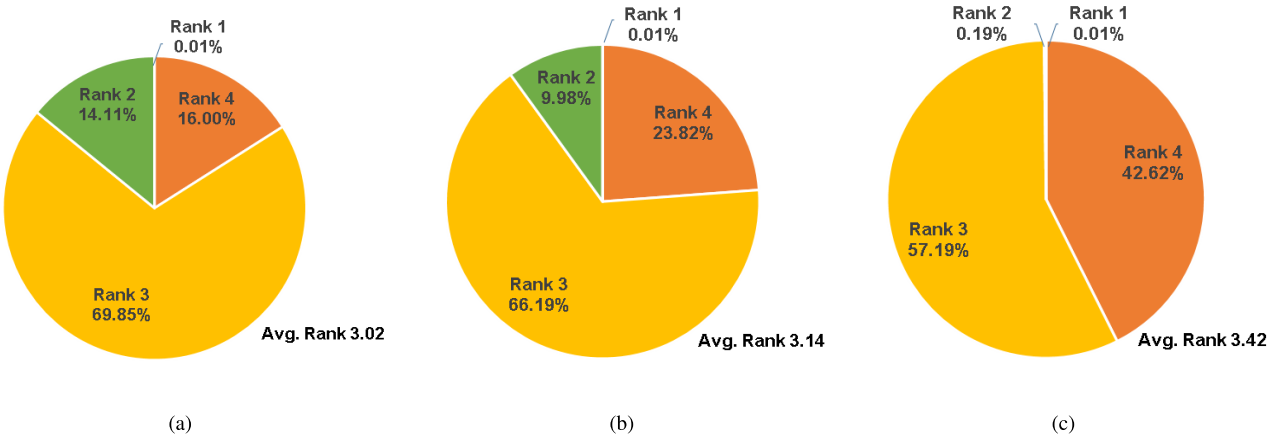

FIGURE 15. Calculated Rank index distribution of (a) Baseline antenna (b) Twin beam same pol. antenna (c) ORPA.

the channels are more like 2×4 MIMO for OPRA and Twin beam system and the SNR strength also diminishes for all configuration.

The average capacity, correlation and rank index over 1 sector $(\alpha/\beta/\gamma)$ of 120°, i.e. $-60°$ to 60°, and 500 m cell radius range, is also calculated and compared for all 3 configuration. The average capacity for all the 3 configuration is compared in bargraph plot, Fig. 12. The proposed OPRA scheme has average capacity of 8.16 bps/Hz compared to 6.26 bps/Hz of baseline scheme. The OPRA achieves 30% higher average capacity from baseline. Similar to capacity, correlation is calculated using (4) and (6) and the average correlation comparison bargraph is shown in Fig. 13. The average correlation of OPRA scheme is slightly higher than the baseline scheme but quite low compare to Twin beam same polarization scheme. The correlation of OPRA is slightly higher than baseline as the beam separation angle compromised for higher capacity with correlation is somewhat at high side. The correlation trade-off for high capacity provide better rank index, i.e. higher rank 4 proportion, in the simulation result, shown next. Percentage of the rank index for baseline, Twin beam same polarization antenna, and OPRA is calculated over $\alpha/\beta/\gamma$ sector from H matrix. The simulated average rank index bar graph comparison is shown in Fig. 14. The detail simulation rank index proportion is shown in pie chart form in Fig.15. The percentage of rank 4 is highest for OPRA scheme, 42.62% in comparison to 16% and 23.82% of baseline and Twin beam scheme, respectively. The average rank index of OPRA is also higher than other configurations, 3.42 in comparison to 3.02 and 3.14 of baseline and twin beam scheme, respectively. The rank index therefore could highlight the improvement in capacity and the throughput of the network, which is utilized in next section for OPRA performance verification because direct measure of network throughput was difficult. These results signify the usages of orthogonal polarization reuse for enhancing channel capacity.

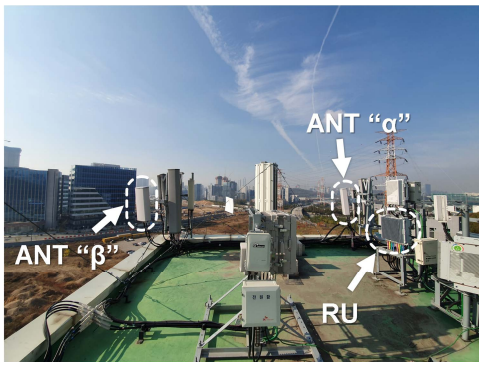

FIGURE 16. Base station antennas on the roof of a building.

VI. FIELD TRIAL TEST AND RESULT

A field test in 5G NR environment with the three types of the antenna system (baseline antenna system, Twin beam same cross-pol. antenna system, and OPRA) to verify the channel capacity and benefits of OPRA over other antenna configuration has been performed. For the field test a small area near KMW headquarter in Hwaseong-si, South Korea is chosen. The BS antenna is set up at the rooftop of a building with radio units, shown in Fig. 16. BS antenna covering sector α and sector β are marked in the figure along with radio unit (RU) for these two BS antennas. The BS is designed and fabricated for the measurement purpose only, where the dual beam is achieved simply by rotation of antenna panel, Fig. 2. The measurement is performed at multiple specific locations using the user equipment Galaxy Note 10 5G around the street of sectors covered by the BS mounted on the rooftop of a building. Galaxy Note 10 5G specified to work for 5G NR 4×4 MIMO network. The measurement was repeated at selected specific locations for all three types of antenna systems. R&S scanner and Diagnostic Monitor with OPTicS tool provided by Innowireless used to monitor the quality of the 5G cellular network received by UE. RSRP, Rank Index, SINR etc. were measured, however, throughput could not be measured. Some of the field test environment

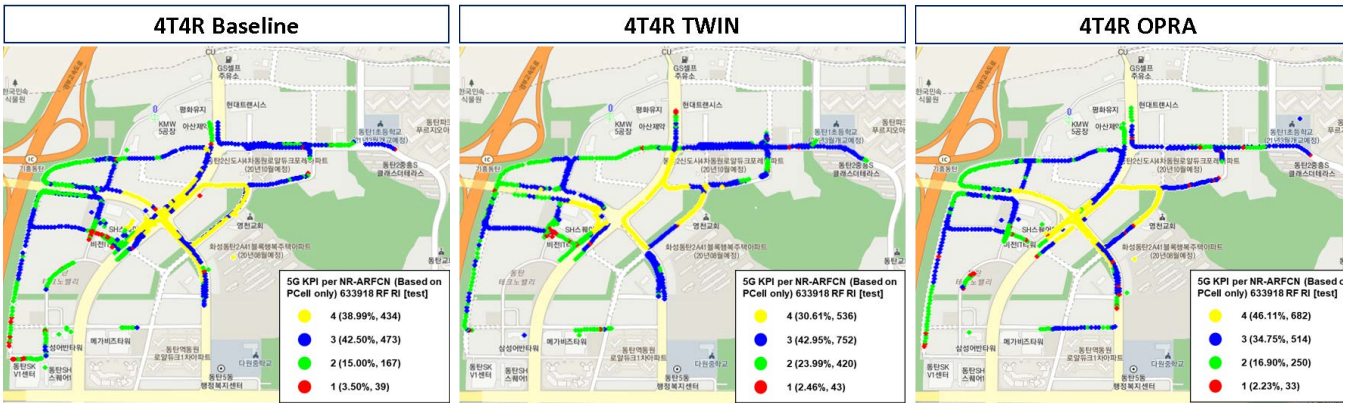

FIGURE 17. Rank Index measurement around base station for (a) Baseline antenna (b) Twin beam same pol. antenna (c) ORPA.

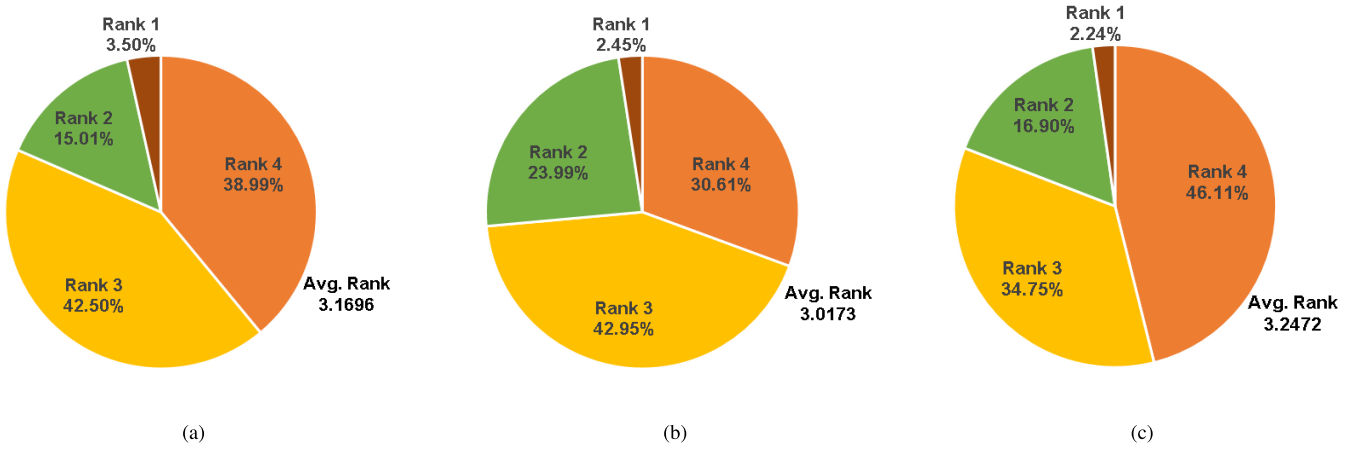

FIGURE 18. Measured Rank index proportion of (a) Baseline antenna (b) Twin beam same pol. antenna (c) ORPA.

TABLE 2. Test environment specification and details.

	Type	Detail Specification
Environment	5G NR	Band 78
		BW 100 MHz
		SCS 30 KHz
		PCI 577
		NR ARFCN 633918
		Freq 3508.77 MHz
Test terminal	Galaxy Note 10 5G	SM-N971N, Exynos
		Android 9
		version N971NKOU1ASK1
Analysis tool	R&S scanner	TSME6, ROMES4 19.2
	Innowireless Optics-S	03.6.0.22N
	Innowireless Analyzer	D5.23.6.6

and tool details used in measurement are tabulated in Table 2.

The application of multiple orthogonal polarization reuse with MIMO aimed at achieving multiple independent channels and minimizing correlation due to polarization orthogonality. The measured signals at different location are analyzed to obtain rank index of the network to compare the

TABLE 3. Simulated and measured rank index.

	OPRA		Twin beam same pol.		Baseline	
	Simul.	Meas.	Simul.	Meas.	Simul.	Meas.
Rank 1	0.01	2.24	0.01	2.45	0.01	3.5
Rank 2	0.19	16.9	9.98	23.99	14.11	15.01
Rank 3	57.19	34.75	66.19	42.95	69.85	42.5
Rank 4	42.62	46.11	23.82	30.61	16	38.99
Avg Rank	3.42	3.25	3.14	3.02	3.02	3.17

TABLE 4. Rank index at measurement points over overlapping zone.

	OPRA	Twin beam same pol.	Baseline Ant.
#1	2.69	2.07	2.75
#8	3.07	2.62	2.75
#9	2.77	2.08	2.54
#10	3.46	2.08	3.21
#11	3.15	2.13	3.15
#12	3.07	2.54	2.77
#13	3.25	2.92	3.07
#14	2.92	2.17	2.58
#18	3	2.5	3
#19	3.86	2.23	3.46

capacity with independent data streams in the network. The rank index (rank 1, rank 2, rank 3, and rank 4) distribution

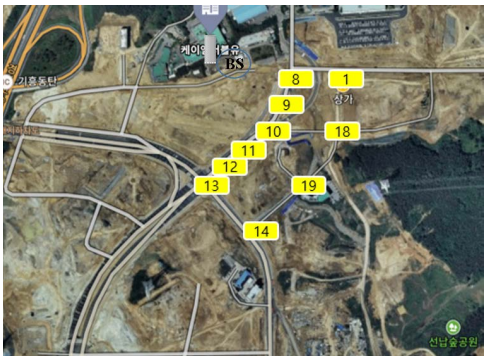

FIGURE 19. Satellite map of measurement area with measurement location over overlapping zone.

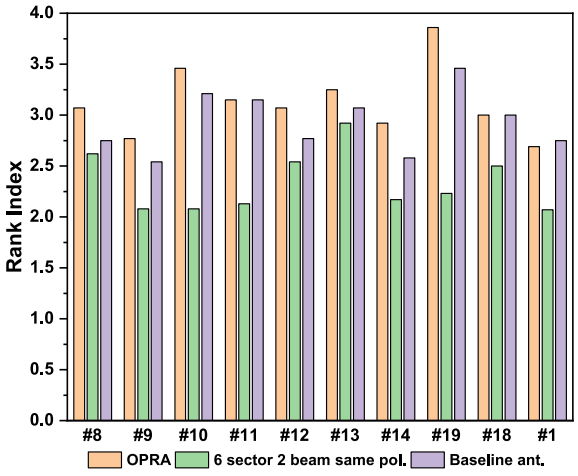

FIGURE 20. Bar graph of the measured rank index over overlapping zone for different BS antenna configuration.

for baseline, Twin beam same polarization, and OPRA configuration is shown over the map of the measurement area in Fig. 17. The portion of yellow mark, representation of rank 4, is more for OPRA system compared to baseline and twin beam same polarization configuration by 18.26% and 50.6%, respectively. The location of BS at the KMW is marked over the map. Similar to the simulation results, the measured rank proportion over the sector for different BS antenna configuration is shown in the pie chart, Fig. 18 for comparison and clarity. The measured and simulated rank index proportion over a sector is tabulated in Table 3. There is slight variation in simulation and measured values because the similarity of scaterrer model employed for simulation and the real dense urban environment are not exactly same, however, the proportion trend calculated is similar to the measured rank index proportion. The rank 4 index proportion of OPRA is hihger out of all three configuration and is evident from both simulated and measured field result. The comparison of the 3 differnet antenna configuration covering a sector with different beam pattern (single beam (baseline), Twin beam same polarization, and dual beam with orthogonal polarizaton) are performed under same set of parameters and conditions. The rank 4 proportion increment can be directly link to the enhancement in MIMO capacity. Therefore, the proposed OPRA configuration verified to enhance MIMO capacity.

The overlapping zone of the twin beam in OPRA makes the most difference in the rank index. It was also observed from SNR and capacity plot in the previous section that SNR and capacity were high over range of UE angular position correspond to Twin beam overlapping area. We analyze the measured result closely for the overlapping area in the sector. Fig. 19 shows the satellite map of the measurement area with some measurement point location number over the overlapping zone. The rank index at the measurement location shown in Fig. 19 is tabulated in Table 4. The rank index of OPRA is higher than baseline and Twin beam same polarization at each measurement location with rank index close to 3 or above 3.

VII. CONCLUSION

The proposed OPRA scheme is very practical and economical which induce no additional cost of installation and higher sectorization. OPRA system capacity over a 120° sector is calculated to be 30% higher than the baseline system. The OPRA configuration succeeded enhancing the channel capacity with simultaneous data channel of 4×4 MIMO and maximize the rank 4 proportion for 4×4 MIMO in a network. Rank 4 proportion in OPRA over a sector is 18.26% and 50.6% more than baseline configuration and Twin beam same pol. configuration. The analysis of OPRA and conventional Twin beam same polarization suggest that reforming from 3-beam(/sector) into 6-beam(/sector) cellular network would not be much advantageous, at least in terms of capacity and rank of the data streams, without additional polarization channel and adopting technologies such as orthogonal polarization reuse. In this paper we analyze the horizontal sectorization using OPRA but both horizontal and vertical sectorization using OPRA is possible and through the combination of vertical and horizontal sectorization, OPRA can achieve maximum user capacity or throughput. The dual beam BS antenna panel presented in the paper is developed from 3-sector BS by simply rotating the array panel. This model is designed and manufactured for experiment and verification purpose only. A co-located quad polarized antenna unit is a demand of the proposed state of the art and is under development and possibly will present in the future.

ACKNOWLEDGMENT

The authors would like to thank KMW Members for their support.

REFERENCES

[1] *Mobile Broadband: The Benefits of Additional Spectrum*, Federal Commun. Commission, Washington, DC, USA, Oct. 2010.
[2] Y. Ye, D. Wu, Z. Shu, and Y. Qian, "Overview of LTE spectrum sharing technologies," *IEEE Access*, vol. 4, pp. 8105–8115, 2016.

[3] M. Thurfjell, M. Ericsson, and P. de Bruin, "Network densification impact on system capacity," in *Proc. IEEE 81st Veh. Technol. Conf. (VTC Spring)*, May 2015, pp. 1–5.
[4] J. Liu, M. Sheng, L. Liu, and J. Li, "Network densification in 5G: From the short-range communications perspective," *IEEE Commun. Mag.*, vol. 55, no. 12, pp. 96–102, Dec. 2017.
[5] A. Pattavina, S. Quadri, and V. Trecordi, "Spectral efficiency improvement of enhanced assignment techniques in cellular networks," in *Proc. IEEE Global Telecommun. Conf.*, vol. 2, Feb. 1996, pp. 1031–1035.
[6] R. Atat, L. Liu, J. Ashdown, M. Medley, J. Matyjas, and Y. Yi, "Improving spectral efficiency of D2D cellular networks through RF energy harvesting," in *Proc. IEEE Global Commun. Conf. (GLOBECOM)*, Dec. 2016, pp. 1–6.
[7] S. N. Tayade, "Spectral efficiency improving techniques in mobile femtocell network: Survey paper," *Proc. Comput. Sci.*, vol. 78, pp. 734–739, Jun. 2016. [Online]. Available: http://www.sciencedirect.com/science/article/pii/S187705091600048X
[8] G. J. Foschini and M. J. Gans, "On limits of wireless communications in a fading environment when using multiple antennas," *Wireless Pers. Commun.*, vol. 6, no. 3, pp. 311–335, Mar. 1998. [Online]. Available: https://link.springer.com/article/10.1023/A:1008889222784
[9] E. Telatar, "Capacity of multi-antenna Gaussian channels," *Eur. Trans. Telecommun.*, vol. 10, pp. 585–595, Nov. 1999. [Online]. Available: https://onlinelibrary.wiley.com/doi/abs/10.1002/ett.4460100604
[10] D. Gesbert, M. Shafi, D. Shiu, P. J. Smith, and A. Naguib, "From theory to practice: An overview of MIMO space-time coded wireless systems," *IEEE J. Sel. Areas Commun.*, vol. 21, no. 3, pp. 281–302, Apr. 2003.
[11] A. Wacker, J. Laiho-Steffens, K. Sipila, and K. Heiska, "The impact of the base station sectorisation on WCDMA radio network performance," in *Proc. 21st Century Commun. Village VTC–Fall, IEEE VTS 50th Veh. Technol. Conf.*, vol. 5, Sep. 1999, pp. 2611–2615.
[12] H. Huang, O. Alrabadi, J. Daly, D. Samardzija, C. Tran, R. Valenzuela, and S. Walker, "Increasing throughput in cellular networks with higher-order sectorization," in *Proc. Conf. Rec. 44th Asilomar Conf. Signals, Syst. Comput.*, Nov. 2010, pp. 630–635.
[13] R. Joyce, D. Morris, S. Brown, D. Vyas, and L. Zhang, "Higher order horizontal sectorization gains for 6, 9, 12 and 15 sectored cell sites in a 3GPP/HSPA+ network," *IEEE Trans. Veh. Technol.*, vol. 65, no. 5, pp. 3440–3449, May 2016.
[14] M. U. Sheikh, K. Ruttik, and R. Jäntti, "Performance analysis of vertical and higher order sectorization in urban environment at 28 GHz," in *Proc. 26th Int. Conf. Telecommun. (ICT)*, Apr. 2019, pp. 335–339.
[15] E. G. Larsson, O. Edfors, F. Tufvesson, and T. L. Marzetta, "Massive MIMO for next generation wireless systems," *IEEE Commun. Mag.*, vol. 52, no. 2, pp. 186–195, Feb. 2014.
[16] K. Nishimori, "Novel technologies using massive MIMO transmission toward 5G and its beyond systems," in *Proc. Int. Symp. Antennas Propag. (ISAP)*, 2018, pp. 1–2.
[17] F. Challita, P. Laly, M. Yusuf, E. Tanghe, W. Joseph, M. Liénard, D. P. Gaillot, and P. Degauque, "Massive MIMO communication strategy using polarization diversity for industrial scenarios," *IEEE Antennas Wireless Propag. Lett.*, vol. 19, no. 2, pp. 297–301, Feb. 2020.
[18] P. Kyritsi, D. C. Cox, R. A. Valenzuela, and P. W. Wolniansky, "Effect of antenna polarization on the capacity of a multiple element system in an indoor environment," *IEEE J. Sel. Areas Commun.*, vol. 20, no. 6, pp. 1227–1239, Aug. 2002.
[19] N. K. Das, T. Inoue, T. Taniguchi, and Y. Karasawa, "An experiment on MIMO system having three orthogonal polarization diversity branches in multipath-rich environment," in *Proc. IEEE 60th Veh. Technol. Conf. (VTC-Fall)*, vol. 2, Sep. 2004, pp. 1528–1532.
[20] P.-Y. Qin, Y. J. Guo, and C.-H. Liang, "Effect of antenna polarization diversity on MIMO system capacity," *IEEE Antennas Wireless Propag. Lett.*, vol. 9, pp. 1092–1095, 2010.
[21] R. B. Dybdal, S. J. Curry, F. Lorenzelli, and D. J. Hinshilwood, "Multiple polarization communications," in *Proc. IEEE Int. Symp. Antennas Propag.*, Jul. 2012, pp. 1–2.
[22] E. Re and P. Angeletti, "Non-orthogonal polarization reuse in multibeam satellite systems," in *Proc. 32nd AIAA Int. Commun. Satell. Syst. Conf.*, San Diego, CA, USA, Aug. 2014. [Online]. Available: https://arc.aiaa.org/doi/abs/10.2514/6.2014-4326
[23] F. Quitin, "Channel modeling for polarized mimo systems/modélisation de canal pour systèmes MIMO polarisés," Ph.D. dissertation, Université Libre de Bruxelles, Brussels, Belgium, 2011.
[24] M. T. Dao, V. A. Nguyen, Y. T. Im, S. O. Park, and G. Yoon, "3D polarized channel modeling and performance comparison of MIMO antenna configurations with different polarizations," *IEEE Trans. Antennas Propag.*, vol. 59, no. 7, pp. 2672–2682, Jul. 2011.
[25] H. Xu, D. Chizhik, H. Huang, and R. Valenzuela, "A generalized space-time multiple-input multiple-output (MIMO) channel model," *IEEE Trans. Wireless Commun.*, vol. 3, no. 3, pp. 966–975, May 2004.
[26] L. Jiang, L. Thiele, and V. Jungnickel, "On the modelling of polarized MIMO channel," in *Proc. Europ. Wireless*, 2007, pp. 1–4.
[27] C. Oestges, V. Erceg, and A. J. Paulraj, "Propagation modeling of MIMO multipolarized fixed wireless channels," *IEEE Trans. Veh. Technol.*, vol. 53, no. 3, pp. 644–654, May 2004.
[28] J. Wang, J. Zhao, and X. Gao, "Modeling and analysis of polarized MIMO channels in 3D propagation environment," in *Proc. 21st Annu. IEEE Int. Symp. Pers., Indoor Mobile Radio Commun.*, Sep. 2010, pp. 319–323.
[29] M. Shafi, A. L. Moustakas, P. J. Smith, A. F. Molisch, F. Tufvesson, and S. H. Simon, "Polarized MIMO channels in 3-D: Models, measurements and mutual information," *IEEE J. Sel. Areas Commun.*, vol. 24, no. 3, pp. 514–527, Mar. 2006.
[30] M. Shafi, M. Zhang, P. J. Smith, A. L. Moustakas, and A. F. Molisch, "The impact of elevation angle on MIMO capacity," in *Proc. IEEE Int. Conf. Commun. (ICC)*, vol. 9, Jun. 2006, pp. 4155–4160.
[31] K. Mammasis, R. W. Stewart, and J. S. Thompson, "Spatial fading correlation model using mixtures of Von Mises Fisher distributions," *IEEE Trans. Wireless Commun.*, vol. 8, no. 4, pp. 2046–2055, Apr. 2009.
[32] *Study on Channel Model for Frequencies From 0.5 to 100 GHz*, document ETSI 3GPP TR 38.901 Version 17.0.0 Release 17, 2022.
[33] J. R. Hampton, *Introduction to MIMO Communications*. Cambridge, U.K.: Cambridge Univ. Press, 2014.
[34] *Spatial Channel Model for Multiple Input Multiple Output (MIMO) Simulations*, document ETSI, 3GPP TR 25.996 Version 11.0.0 Release, 2017, vol. 11.
[35] H. Asplund, A. A. Glazunov, A. F. Molisch, K. I. Pedersen, and M. Steinbauer, "The COST 259 directional channel model—Part II: Macrocells," *IEEE Trans. Wireless Commun.*, vol. 5, no. 12, pp. 3434–3450, Dec. 2006.

LAXMIKANT MINZ was born in Katihar, India, in September 1986. He received the B.Tech. degree in electronic and communication engineering from the NIT Nagpur, Nagpur, India, in 2007, and the M.Tech. degree in RF and microwave engineering from the IIT Kharagpur, India, in 2009. He is currently pursuing the Ph.D. degree with the School of Electrical Engineering, Korea Advanced Institute of Science and Technology (KAIST). His research interests include antenna design, wireless communications, radar systems, and microwave circuit design.

YE-EUN CHI received the B.S. degree in electronic engineering from Ewha Womans University, Seoul, South Korea, in 2016, and the M.S. degree from the School of Electrical Engineering, Korea Advanced Institute of Science and Technology, Daejeon, South Korea, in 2019, where she is currently pursuing the Ph.D. degree. Her current research interests include the design of millimeter-wave systems, self-calibration systems, and MIMO beamforming.

KYUNGHOON KWON received the B.S. degree in electrical engineering from Sejong University, Seoul, South Korea, in 2010, and the M.S. and Ph.D. degrees in electrical engineering from Korea University, Seoul, in 2012 and 2016, respectively. He is currently a Senior Research Engineer with KMW Inc. His research interests include wireless communications, channel coding theory, and MIMO channel modeling.

MIN-SEON YUN received the B.S. and M.S. degrees in electrical engineering from Konkuk University, Seoul, South Korea, in 1996 and 1998, respectively. He is currently a Managing Director with KMW Inc. His research interests include digital hardware design and digital signal processing.

YOUNG-CHAN MOON received the B.S., M.S., and Ph.D. degrees in electrical engineering from Sogang University, Seoul, South Korea, in 1990, 1992, and 1996, respectively. From 1996 to 2000, he was a Research Engineer at the Electronics and Telecommunications Research Institute (ETRI). He is currently a Chief Technology Officer (CTO) with KMW Inc. His research interests include RF circuit and antenna integrated system design for cellular base station.

DUK-YONG KIM received the B.S. and Ph.D. (Hons.) degrees in electrical engineering from Sogang University, Seoul, South Korea, in 1983 and 2008, respectively. He is currently a Founder and a Chief Executive Officer (CEO) with KMW Inc. His research interests include RF components, filter, and system for mobile communication.

SEONG-OOK PARK (Senior Member, IEEE) was born in Kyungpook, South Korea, in December 1964. He received the B.S. degree in electrical engineering from Kyungpook National University, in 1987, the M.S. degree in electrical engineering from the Korea Advanced Institute of Science and Technology, Daejeon, in 1989, and the Ph.D. degree in electrical engineering from Arizona State University, Tempe, AZ, USA, in 1997. From March 1989 to August 1993, he was a Research Engineer at Korea Telecom, Daejeon, working with microwave systems and networks. He joined the Telecommunication Research Center, Arizona State University, until September 1997. Since October 1997, he has been a Professor with the Korea Advanced Institute of Science and Technology. His research interests include mobile handset antenna, and analytical and numerical techniques in the area of electromagnetics. He is a member of Phi Kappa Phi.